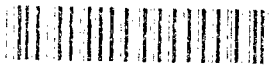

ARMY RESEARCH LABORATORY

DISPERSION EFFECTS ON MILLIMETER WAVELENGTH ATTENUATION EFFICIENCIES FOR A VARIETY OF FIBERS

C. W. Bruce
U.S. Army Research Laboratory

A. V. Jelinek, E. Crosby, and R. Haloren
Physical Science Laboratory

J. Hale
Chemical Research Development and Engineering Center

R. E. Lee, J. Arthur, and E. Zarret
U.S. Army Research Laboratory

ARL-TR-58 August 1993

Approved for public release; distribution unlimited.

NOTICES

Disclaimers

The findings in this report are not to be construed as an official Department of the Army position, unless so designated by other authorized documents.

The citation of trade names and names of manufacturers in this report is not to be construed as official Government indorsement or approval of commercial products or services referenced herein.

Destruction Notice

When this document is no longer needed, destroy it by any method that will prevent disclosure of its contents or reconstruction of the document.

REPORT DOCUMENTATION PAGE

Form Approved
OMB No. 0704-0188

1. AGENCY USE ONLY *(Leave blank)*	2. REPORT DATE	3. REPORT TYPE AND DATES COVERED
	August 1993	Final

4. TITLE AND SUBTITLE

DISPERSION EFFECTS ON MILLIMETER WAVELENGTH ATTENUATION EFFICIENCIES FOR A VARIETY OF FIBERS

5. FUNDING NUMBERS

6. AUTHOR(S)

C. W. Bruce; A. V. Jelinek, E. Crosby, and R. Haloren*; J. Hale†; R. E. Lee, J. Arthur, and E. Zarret‡

7. PERFORMING ORGANIZATION NAME(S) AND ADDRESS(ES)

U.S. Army Research Laboratory
Battlefield Environment Directorate
ATTN: AMSRL-BE
White Sands Missile Range, NM 88002-5501

8. PERFORMING ORGANIZATION REPORT NUMBER

ARL-TR-58

9. SPONSORING/MONITORING AGENCY NAME(S) AND ADDRESS(ES)

U.S. Army Research Laboratory
2800 Powder Mill Road
Adelphi, MD 20783-1145

10. SPONSORING/MONITORING AGENCY REPORT NUMBER

11. SUPPLEMENTARY NOTES

*Physical Science Laboratory, New Mexico State University, Las Cruces, NM; †Chemical Research Development and Engineering Center, Aberdeen Proving Ground, MD; ‡U.S. Army Research Laboratory (SLAD), White Sands Missile Range, NM

12a. DISTRIBUTION/AVAILABILITY STATEMENT

Approved for public release; distribution unlimited.

12b. DISTRIBUTION CODE

13. ABSTRACT *(Maximum 200 words)*

Results of several field experiments have been used to determine extinction efficiencies primarily of graphitic fibers and to relate these efficiencies to length distributions. Of the three dispersion techniques employed, two were driven by constant air pressure and the third dispersed fibers by explosive force. Generally, the latter significantly altered the distribution. When a significant proportion of the fibers was fragmented to lengths shorter than a half wavelength, the efficiency decreased notably. Extinction efficiencies for almost all the explosively dispersed clouds were in this category. For frequencies of 35 GHz and lower, efficiencies for explosive dissemination typically were reduced by factors of 2 to 4. Efficiencies at 94 GHz were much less affected because the ratio of particle length to wavelength remained, on the average, higher than one-half. In contrast, length distributions for fibers cut from spools and immediately disseminated by constant air flow almost always sharply peaked near the cut length and had efficiencies near to that calculated for the cut length. Calculations and measurements are in agreement on this issue.

14. SUBJECT TERMS

Extinction, efficiency, fibrous aerosols

15. NUMBER OF PAGES

17

16. PRICE CODE

17. SECURITY CLASSIFICATION OF REPORT	18. SECURITY CLASSIFICATION OF THIS PAGE	19. SECURITY CLASSIFICATION OF ABSTRACT	20. LIMITATION OF ABSTRACT
Unclassified	Unclassified	Unclassified	SAR

Contents

List of Illustrations

Figures

Tables

1. About the Experiments

A quantitative understanding of the millimeter wavelength attenuative potential (absorption, scattering) for conductive, fibrous aerosols has been sought for a number of years in a joint laboratory experimental and theoretical program (Bruce et al. 1990a, Pedersen et al. 1985, Pedersen et al. 1987, and Waterman and Pedersen 1992). Interest in theoretical solution for straight fibers with finite conductivity and finite length has been growing during the same period as a result of the relationship to antenna problems (Chatterjee et al. 1992, Einarson 1987, and Richmond 1980).

As a concurrent line of research, accurate field measurement systems have been developed to assure that effects of the turbulent atmosphere present no surprises. This report deals with a variety of these latter measurements.

Optical efficiencies (effective cross sections for absorption, total scattering or extinction normalized to particle volume or particle mass) have been measured in situ and/or calculated for generic graphitic fibers. A few results are for fibers with a relatively thick, high conductivity coating of thickness greater than the skin depth. Efficiencies were calculated using measured length and diameter distributions.

For two of the experimental series (series I and II), all measurements (optical and characterization) were performed within a relatively small region roughly central to the continuously generated aerosol cloud. Data for 94 GHz and 35 GHz are represented within these two series. Line integrated data spanning the cloud were obtained for a third series (series III) as that was the only available mode for attenuation measurements at the lower two of the three frequencies used (8 GHz, 17 GHz, and 35 GHz). Both constant air pressure and explosively driven methods of dispersion were used for the third series. Calculations of efficiencies based on measured length distributions for explosively dispersed fibers are presented for a fourth experimental series (series IV).

The instruments used in the series I and II measurements for determining the mass normalized coefficients were so arranged that all would interact with as close as possible to a common body of aerosol. The optical coefficients were measured with short path transmissometers having nearly coincident 3 m path lengths. The path length was chosen to optimize the millimeter wavelength measurement quality (50 percent transmissivity) for the expected source strength. A third nearly coincident optical beam at a visible wavelength (0.63 μm) provided a basis for determining the normalizing aerosol volume factor. Located directly downwind, but central and close to these paths, were several aerosol characterization measurements of point nature: a passive sampling filter (dosimeter), a time resolved particle collector that employs moving tape, a nephelometer sampling a relatively large instantaneous volume for obtaining valid statistics in short intervals, and a windspeed-matched active sampling system using a sensitive differential pressure sensor. Figure 1 shows the arrangement. The somewhat redundant but unique set of measurements and subsequent analysis provide fiber length and diameter distributions, variations in time, and an independent determination of the aerosol density for normalization of the millimeter wavelength extinction coefficients.

The passive sampling filter device used a mesh that was shown in wind tunnel studies not to form a significant aerodynamic barrier to the impinging fibers unless heavily loaded. In the latter case, the passive device does form a strong barrier and most of the fibers will circumvent the sampler. The active sampling device measures the airflow through the filter and compares it against the ambient windspeed. Isokineticity (wind-matched airflow) through the filter can therefore be maintained until the system is truly choked. The particle collector is, in effect, a calibrated barrier; it is calibrated as a function of windspeed. Congestive effects for this instrument are not significant. The nephelometer, as designed for these measurements, used straight-through, unobstructed flow with a detection angle centered about 90° and a detection volume of about 30 cc. Nephelometers were also used to enhance the time resolution of the particle collector and transmissometer data.

The experiments of Series III were performed with three microwave beams and the additional HeNe geometrical characterization beam as nearly coincident as possible. The 35 GHz and 0.63 μm crosswind beams were transmitted between towers spaced by 100 m. For the other two wavelengths, 8 GHz and 17 GHz, radar receivers were used with large mobile dish antennas adjacent to one tower and transmitters on the opposite tower. The approximate height of the line(s) of sight was 15 ft, the minimum value for avoidance of multipath and ground clutter. The beams intersected vertically in the central portion of the path while having as much as several meters displacement horizontally. Time-displacement corrections were performed later to correlate the various signals.

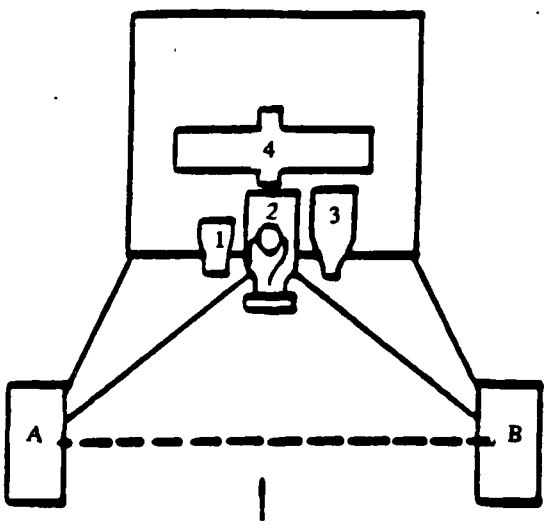

Figure 1. Top view of system for measurement of extinction efficiencies. Three transmissometer beams pass between platforms "A" and "B." Each platform includes a millimeter wavelength transmitter and receiver at different wavelengths in a closed, nonabsorbing container. Aerosol characterization devices shown are: (1) passive filter-mesh sampler, (2) active isokinetic sampler with differential airflow sensor, (3) Particle Collector, and (4) nephelometer.

Mesh filters and a linear array of nephelometers produced the geometrical characterization and transverse density profiles for the clouds. The primary purpose of the nephelometer array was to indicate the cloud location with respect to the intersection region rather than as a basis for absolute calculations.

The series III experiment was clearly less definitive than the previous two and more assumptions were made in the analyses. Nevertheless, it was made worthwhile for three important reasons. It was the only optical experiment to include metallic (high conductivity) fibers and explosive dissemination. Also, the additional (lower) frequencies extended the measurements of extinction efficiencies for these fibers into a new (lower) domain.

2. Results

Time histories of the extinction coefficients for the series I and II experiments, those obtained from the line-integrated short path transmissometers and the time resolved aerosol characterization "point" measurements, all show a high degree of correlation within the response bandwidth (DC to about 1 Hz). This strongly suggests that these coefficients are all linearly related to the aerosol mass density. The volume or mass normalized coefficients are thus essentially constant in time for a given experiment, that is, for a given aerosol composition and size distribution.

Use of the visible laser beam to compute the aerosol line density geometrically (fiber diameter $>>$ wavelength) yields the most comparable measure for mass normalization of the microwave extinction coefficients. The time averages of the series I extinction efficiencies and their test-by-test RMS variations for each of the four aerosol categories (two frequencies/two diameters) are listed and compared with the theoretical values at the cut length in table 1. The length distributions were quite narrow, as indicated by typical distribution variances about deviation of $\sigma = 0.2$ mm. The quantity of information for the different trials varied greatly; so the authors have used weighting factors in forming the averages.

Clumping or binding together of fibers was minimal, and theory applied to measured distributions of bundles also indicates minimal effects (less than 5 percent) on the efficiencies. Distributions of multiples closely approximated a single decreasing power law for all trials; the probability of encountering a bundle of 10 was about 10^{-3}.

Radiation for both of the microwave systems was vertically polarized for experimental series I and II, so the question arises as to whether the particles were randomly oriented. A simultaneous independent measurement using vertical and horizontal 0.63 μm laser beams detected little tendency, on the average, for the fibers to orient in the ambient turbulence for this experimental series.

Table 1. Millimeter Wavelength Extinction Efficiencies, $\epsilon(m^2/g)$, for Individual Experiments of Series I.

Experiment No.	ϵ @ 35 GHz	ϵ @ 94 GHz
1	1.46	1.47
2	1.70	1.61
3	1.62	1.64
4	1.66	1.46
5	2.20	1.60
6	2.93	2.73
7	2.38	1.49
8	3.12	2.69
9	2.15	1.93
10	2.94	2.62

Table 2 shows that all but one of the mean efficiencies for series I are in good agreement with the calculated values although the variation from trial-to-trial can be significant. There is also agreement that the extinction mass efficiency at 35 GHz is higher than for 94 GHz. Finally, note that there is general agreement on the effect of the particle diameter; that is, the smaller diameter particles have higher efficiencies.

Table 2. Mean Measured and Theoretical Extinction Mass Efficiencies Compared for Series I Experiments.

	Measurement/Theory $[m^2g^{-1}]$	
Wavelength (cm)	6.5 μm diameter	3.8 μm diameter
0.319	1.53 $\pm$ 6% / 1.42	2.25 $\pm$ 26% / 2.06
0.857	1.61 $\pm$ 7% / 2.15	2.64 $\pm$ 16% / 2.50

Basically the same measurements were made for the series II experiments except that both horizontal and vertical polarizations of E field were measured at 35 GHz (and averaged for this report). Ninety-four GHz was not used. Results are again tabulated (table 3) by experiment and this time are compared with calculations based on the length distributions for each experiment. Also included in this table are the efficiencies at cut lengths. Figure 2 shows sample length distributions.

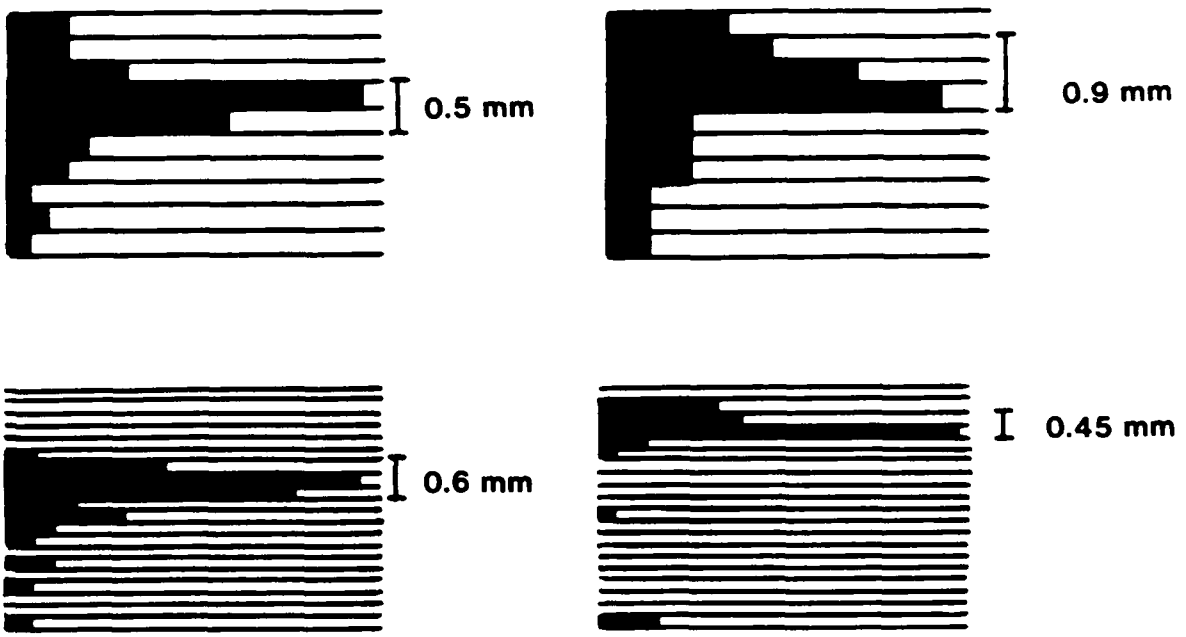

Figure 2. Sample length distributions for experimental series II. Distribution is on the vertical axis and the relative amplitude is on the horizontal axis in all cases. The span is indicated for roughly 50 percent points on bar graph. Sigma is considerably less.

Table 3. Measured and Calculated Extinction Efficiencies $\epsilon(m^2g^{-1})$ @ 35 GHz for Individual Experiments of Series II.

Experiment	Measured $<\epsilon>$	Calculated ϵ_{CL}	Calculated ϵ_{dist}
1	1.75	2.16	1.92
2	1.49	2.17	2.00
3	2.34		1.76
4	1.80	2.01	1.55
5	2.17	2.01	1.68
6	2.33	2.01	2.02
7	2.09	1.78	1.80
8	1.68	1.78	1.80
9	1.71	1.78	1.76

The results show that the measured extinction efficiencies for the airborne cloud are close to cut length ideal. The averaged measured efficiency is 96 percent of that for the cut length. We also note a 4 percent difference* between the measured and calculated averages (calculated is lower) while the measured intertrial standard deviation is about 17 percent. The standard deviation of the difference between measured and calculated values is also about 17 percent. Uncertainties are principally in the HeNe measurement (estimate 5→8 percent/trial, average) and length distribution (estimate 10→15 percent on the calculated values). A differential error analysis indicates that the variation could be accounted for by the uncertainties.

$$\Delta\epsilon = \left(\frac{\Delta\rho}{\rho} + \frac{\Delta R}{R} + \frac{\Delta\epsilon_{mmw}}{\epsilon_{mmw}} + \frac{\Delta\epsilon_{0.6}}{\epsilon_{0.6}}\right)\left(\rho R\frac{\epsilon_{mmw}}{\epsilon_{0.6}}\right)$$

$$= 0.02 + 0.05 + 0.03 + 0.08$$

$$\approx 18\%$$

where ρ, R, ϵ_{mmw} and $\epsilon_{0.6}$ are the aerosol bulk density, radius and the mass normalized extinction cross sections.

The technique employed for the series III experiments involved a more compromised geometry (as we discussed earlier) in order to accommodate the equipment available for the two lower frequencies. The principal consequence of this compromise was a reduction in the time-correlation of the different signals.

Examples of the reduced correlation can be seen by comparing figures 3a and 3b. Figure 3a shows time correlation for the nearly collinear short path transmissometers of experimental series I and II while figure 3b shows some of the more closely correlated time histories of the series III experiments. Others had to be rejected for lack of time correlation. The amount of data lost was not serious and perhaps is a valuable reminder that data from different total-traverse paths may not be comparable. While every effort was made to bring all beams into proximity for the series III experiments, this is not often the case when results from different transmissometers are compared.

Accurate length distributions were difficult to obtain for this series since the fibers would mat together (particle collector was not used for this series) and lifting samples from the filter using transparent adhesive material did not necessarily give representative distributions. Therefore, since good agreement with the theory for other series has been the rule, only examples of the different materials/cuts were calculated for series III.

---

*Particle distributions for two experiments appeared to include fibers broken during the measurement. In such cases, the tape showed split fibers. When these two distributions (2, 4) are removed, the measured and calculated averages agree to about 1 percent.

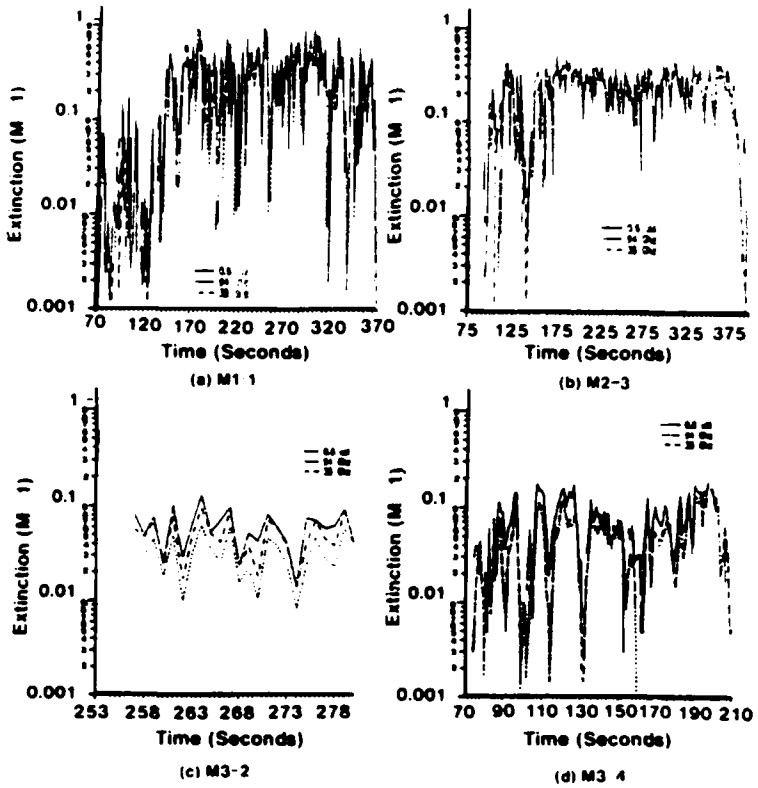

Figure 3a. Extinction coefficients for optical measurements of series I and II experiments. Typical traces. One trace (0.6 μm) is boosted one order of magnitude.

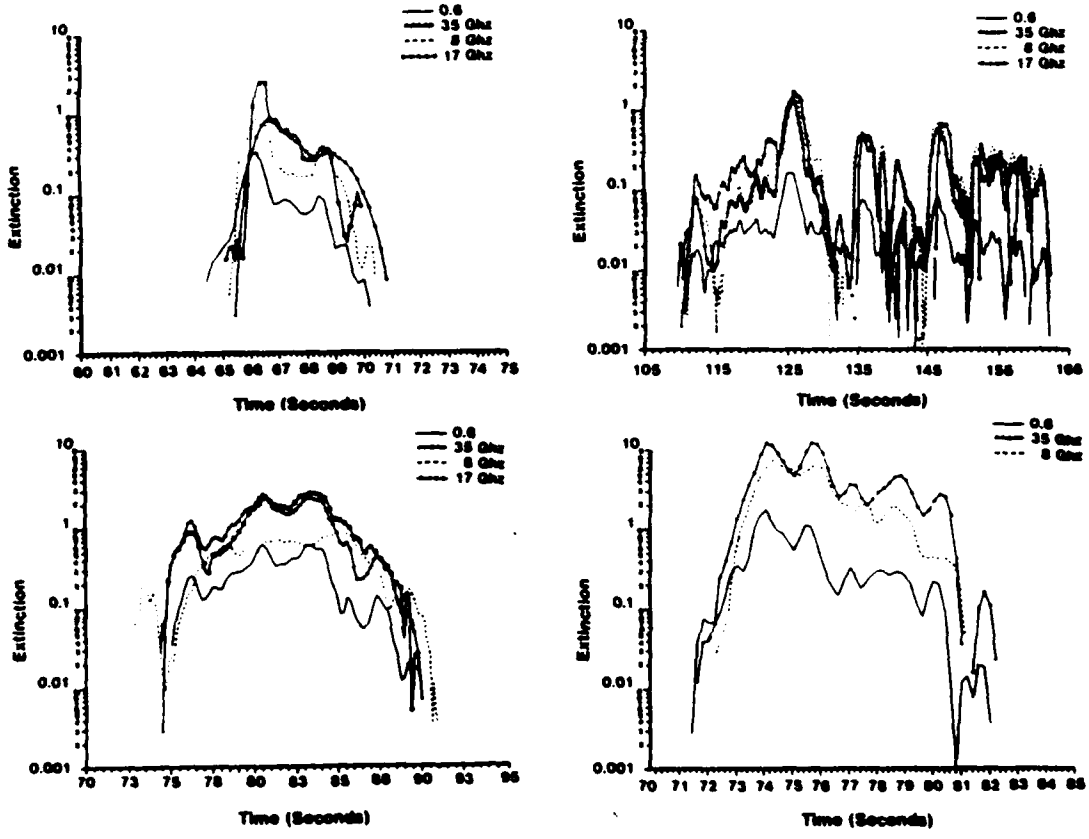

Figure 3b. Correlation with time for four signals of series III experiments. In this case, plots are for the best available correlations. In the other extreme, some did not even bear strong resemblance.

The results of table 4 indicate that, when dispersed explosively, the efficiencies of the graphitic fibers are typically reduced by more than a factor of two. This is in line with results for other series. The lowest frequency exhibits reduced efficiencies since a larger proportion of the fibers is shorter than a half wavelength.

Table 4. Extinction Efficiencies for Explosively Dispersed Fibers.

Trial No.	Cut Length (in)	Fiber Diameter (μm)	Composition G-Graphite N_iG Nickel Coated	Signal Correlation Quality	Extinction Efficiencies (measured/calculated) (m^2/g)		
					8 GHz	17 GHz	35 GHz
1	1/4	3.6	G	Good	0.63/	1.46/	1.36
					0.93	1.51	1.96
			(cut length)		2.37	2.62	2.56
2	1/4	7.9	G	Good	0.48/	1.08/	0.68/
					0.49	1.17	1.06
			(cut length)		0.81	2.22	1.90
3	1/4	7.9	G	Good	0.54	0.94	0.80
4	1/4	7.9	G	Good	0.58	---	0.84
5	1/4	7.9	G	Fair	0.58	---	0.48
6*	1/2	8.3	G	Good	0.64	1.58	1.42
7	1/4	9.2	Ni-G	Good	0.08/	1.12/	0.48
					0.02	0.77	1.29
			(cut length)		1.51E-2	0.86	1.00
8	1/4	9.2	Ni-G	Good	low	0.81	1.90
9	1/2	9.2	Ni-G	Good	0.74	1.25	0.99
			(cut length)		0.90	1.80	3.77
10	1/2	9.2	Ni-G	Good	1.19	0.77	0.89
11	1/2	9.2	Ni-G	Good	---	0.85	0.68
12	1/2	9.2	Ni-G	Fair	0.80	1.23	0.53

*Constant generation, not explosively dispersed.

The nickel-coated fibers strongly show the reduced efficiency when the fiber lengths are on the short side of the prime resonance. Other length-dependent features are smeared by the breadth of the distribution. None of the available wavelengths provides the prime resonance at the cut lengths of the nickel-coated fibers.

Because of the known sensitivity of the visible and near-IR detectors to small particles, it was understood that any residue of the explosive used for dispersal of the fibers would be quite measurable. This signal would appear only in the normalization of the microwave extinction coefficients, causing a proportional error (apparent reduction) in the efficiencies. This effect was investigated by removing all the fibers from several explosive units and performing the experiment otherwise in the same fashion. Our concern was affirmed but the magnitude varied from little to tens of percent change in efficiency. Statistical analysis was not possible, so significant errors may be present in the measured results of this series. Nevertheless, the presence of the contaminants is not apparent in the results (note, for example, relationship with calculated values).

The explosive manner of dispersion for the fourth series of experiments produces length distributions that show no peak at all at the cut length - if they are cut (some are not). These distributions, as seen in the examples of figure 4, show only a tail at the longer lengths and peak at lengths having very small cross sections per unit mass.

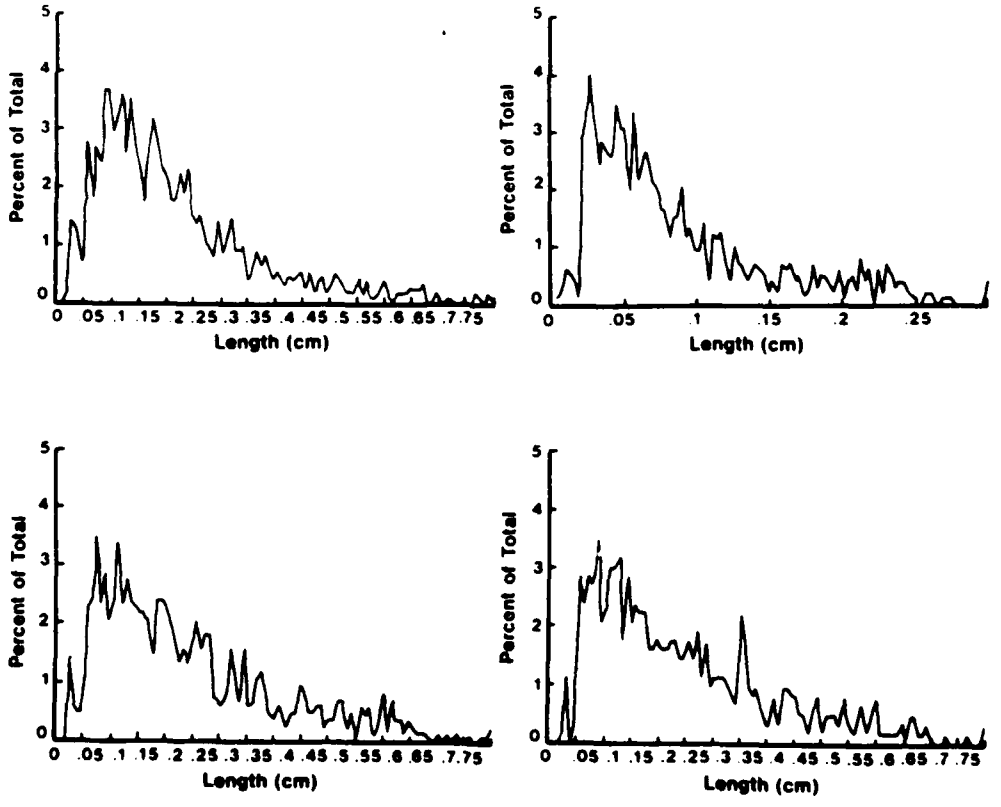

Figure 4. Examples of the length distributions for the explosive-only series IV experiments. These have no peaks at the cut-lengths while those of the series III experiments did show at least a definable peak at the cut length. Yet the calculated extinction efficiencies are not very different.

What happens to the efficiencies in such cases? Table 5 gives calculated values. All these trials were for graphite. The average extinction efficiency @ 35 GHz is about 40 percent (±25 percent) of that attainable with the ideal cut length. The continuous air dispersion experiments, by comparison, produce extinction efficiencies that, for graphite, are those of the cut lengths to within a few (<5) percent.

Table 5. Calculated Extinction Efficiencies Using Length Distributions, Average Diameters and an Electrical Conductivity of 7 X 10^4 mho/m.

Event	Diameter	ϵ_{35}	$\epsilon(m^2/9)$ ϵ_{94}	ϵ_{94}
6-12	6.67	0.82	1.00	2.31
7-12	6.89	0.89	1.12	2.30
7-10	6.67	0.92	1.02	2.31
6-13	6.78	0.41	0.68	2.31
7-17	6.82	1.08	1.18	2.30
8-3	6.91	0.68	0.93	2.30
7-15	6.82	0.96	1.16	2.30
6-15	6.97	0.45	0.78	2.29
8-7	6.95	1.11	1.11	2.29
6-11	6.89	1.02	1.12	2.30
6-10	7.00	1.06	1.04	2.29
8-5	6.64	0.98	1.13	2.32
8-1	6.86	1.04	1.18	2.30
8-2	6.71	0.79	1.08	2.31
7-1	7.04	0.73	1.02	2.29

$<\epsilon_{35}>$ = 0.86 ± 25% $m^2/9$
$<\epsilon_{94}>$ = 1.04 ± 13% $m^2/9$
$<\epsilon_{35}>$ = 38% of that @ cut length

3. Results and Conclusions

Several specific observations can be made regarding the general results of these trials, and at least one quite relevant question is left unanswered.

First, most of these data are for the graphitic fibers and there is good agreement between the theory and the measurements on the values of the extinction efficiencies.

Agreement between measurement and theory extends, as expected, to a range of frequencies (8 GHz to 140 GHz (140 GHz not presented here)) for the actual field measurements. Since graphites exhibit no quantum structure anomalies anywhere in the millimeter/microwave wavelength bands, parameters of the calculations, for example, electrical conductivity, electron relaxation rate and mean free path, the accuracy of the calculations seems secure at frequencies within this range.

As dispersed in continuous fashion, the extinction efficiencies of the particles that appear beyond the "source" or generation region are very nearly those of the cut length. This is confirmed by calculations based on measurements of the distributions.

Clearly the explosive dispersion takes a significant toll on the efficiencies of the dispersed aerosol, that is, roughly a factor of two.

The issue left unsettled here is the proportion of aerosol that is effectively separated and made airborne for extended distances.

Lastly, nickel, which we have confirmed by laboratory measurements and comparisons with theory to be much more efficient than graphite when cut at the prime resonance, does not show its maximum attenuation when cut between frequencies of the illuminating radiation. Only the "Rayleigh" particles (actually, $(kL/2 < 1)$ really reveal any strong spectral feature of the high conductivity particles. For the length weighted average attenuation, the nickel-coated particles are still off resonance and yield about the same efficiency as the graphitic ones.

Literature Cited

Bruce, C. W., D. R. Ashmore, P. C. Pittman, N. E. Pedersen, J. C. Pedersen, and P. C. Waterman, 1990a, "Attenuation at a Wavelength of 0.86 cm Due to Fibrous Aerosols, Appl Phys Letters, 56:791.

Chatterjee, A., J. L. Volakis, and W. J. Kent, 1992, "Scattering by a Perfectly Conducting and a Coated Thin Wire Using a Physical Basis Model," IEEE Transaction on Antennas and Propagation, 40:761-769.

Einarson, O., 1987, Electromagnetic and Acoustic Scattering by Simple Shapes, Bowman et al. (ed), Hemisphere, New York.

Richmond, J. H., 1980, "Greens Function Technique for Near Zero Scattering by Cylindrical Wires of Finite Conductivity," IEEE Transaction on Antennas and Propagation, AP-28, 114-117.

Pedersen, N. E., J. C. Pedersen, and P. C. Waterman, 1985, Absorption and Scattering by Conductive Fibers: Basic Theory and Comparison with Asymtotic Results, USAF Contract Report F49620-84-C-0045, Air Force Office of Scientific Research, building 410, Bolling Air Force Base, Washington, DC 20332-6448.

Pedersen, N. E., P. C. Waterman, and J. C. Pedersen, 1987, Absorption Scattering and Thermal Radiation by Conductive Fibers, USAF Contract Report F49620-84-C-0045, Air Force Office of Scientific Research, building 410, Bolling Air Force Base, Washington, DC 20332-6448.

Waterman, P. C., and J. C. Pedersen, 1992, Scattering by Finite Wires, Appl Phys, 72:349-357.

DISTRIBUTION LIST FOR PUBLIC RELEASE

Commandant
U.S. Army Chemical School
ATTN: ATZN-CM-CC (S. Barnes)
Fort McClellan, AL 36205-5020

NASA/Marshall Space Flight Center
Deputy Director
Space Science Laboratory
Atmospheric Sciences Division
ATTN: ES01 (Dr. George H. Fichtl)
Huntsville, AL 35812

NASA/Marshall Space Center
ATTN: Code ES44 (Dale Johnson)
Huntsville, AL 35812

NASA/Marshall Space Flight Center
Atmospheric Sciences Division
ATTN: Code ED-41
Huntsville, AL 35812

Deputy Commander
U.S. Army Strategic Defense Command
ATTN: CSSD-SL-L
Dr. Julius Q. Lilly
P.O. Box 1500
Huntsville, AL 35807-3801

Commander
U.S. Army Missile Command
ATTN: AMSMI-RD-AC-AD
Donald R. Peterson
Redstone Arsenal, AL 35898-5242

Commander
U.S. Army Missile Command
ATTN: AMSMI-RD-AS-SS
Huey F. Anderson
Redstone Arsenal, AL 35898-5253

Commander
U.S. Army Missile Command
ATTN: AMSMI-RD-AS-SS
B. Williams
Redstone Arsenal, AL 35898-5253

Commander
U.S. Army Missile Command
ATTN: AMSMI-RD-DE-SE
Gordon Lill, Jr.
Redstone Arsenal, AL 35898-5245

Commander
U.S. Army Missile Command
Redstone Scientific Information Center
ATTN: AMSMI-RD-CS-R/Documents
Redstone, Arsenal, AL 35898-5241

Commander
U.S. Army Intelligence Center and Fort Huachuca
ATTN: ATSI-CDC-C (Mr. Colanto)
Fort Huachuca, AZ 85613-7000

Northrup Corporation
Electronics Systems Division
ATTN: Dr. Richard D. Tooley
2301 West 120th Street, Box 5032
Hawthorne, CA 90251-5032

Commander - Code 3331
Naval Weapons Center
ATTN: Dr. Alexis Shlanta
China Lake, CA 93555

Commander
Pacific Missile Test Center
Geophysics Division
ATTN: Code 3250 (Terry E. Battalino)
Point Mugu, CA 93042-5000

Lockheed Missiles & Space Co., Inc.
Kenneth R. Hardy
Org/91-01 B/255
3251 Hanover Street
Palo Alto, CA 94304-1191

Commander
Naval Ocean Systems Center
ATTN: Code 54 (Dr. Juergen Richter)
San Diego, CA 92152-5000

Meteorologist in Charge
Kwajalein Missile Range
P.O. Box 67
APO San Francisco, CA 96555

U.S. Department of Commerce
Mountain Administration Support
Center
Library, R-51 Technical Reports
325 S. Broadway
Boulder, CO 80303

Dr. Hans J. Liebe
NTIA/ITS S 3
325 S. Broadway
Boulder, CO 80303

NCAR Library Serials
National Center for Atmos Rsch
P.O. Box 3000
Boulder, CO 80307-3000

HQDA
ATTN: DAMI-POI
Washington, DC 20310-1067

Mil Asst for Env Sci Ofc of
The Undersecretary of Defense
for Rsch & Engr/R&AT/E&LS
Pentagon - Room 3D129
Washington, DC 20301-3080

HQDA
DEAN-RMD/Dr. Gomez
Washington, DC 20314

Director
Division of Atmospheric Science
National Science Foundation
ATTN: Dr. Eugene W. Bierly
1800 G. Street, N.W.
Washington, DC 20550

Commander
Space & Naval Warfare System Command
ATTN: PMW-145-1G (LT Painter)
Washington, DC 20362-5100

Commandant
U.S. Army Infantry
ATTN: ATSH-CD-CS-OR
Dr. E. Dutoit
Fort Benning, GA 30905-5090

USAFETAC/DNE
Scott AFB, IL 62225

Air Weather Service
Technical Library - FL4414
Scott AFB, IL 62225-5458

USAFETAC/DNE
ATTN: Mr. Charles Glauber
Scott AFB, IL 62225-5008

Commander
U.S. Army Combined Arms Combat
ATTN: ATZL-CAW (LTC A. Kyle)
Fort Leavenworth, KS 66027-5300

Commander
U.S. Army Space Institute
ATTN: ATZI-SI (Maj Koepsell)
Fort Leavenworth, KS 66027-5300

Commander
U.S. Army Space Institute
ATTN: ATZL-SI-D
Fort Leavenworth, KS 66027-7300

Commander
Phillips Lab
ATTN: PL/LYP (Mr. Chisholm)
Hanscom AFB, MA 01731-5000

Director
Atmospheric Sciences Division
Geophysics Directorate
Phillips Lab
ATTN: Dr. Robert A. McClatchey
Hanscom AFB, MA 01731-5000

Raytheon Company
Dr. Charles M. Sonnenschein
Equipment Division
528 Boston Post Road
Sudbury, MA 01776
Mail Stop 1K9

Director
U.S. Army Materiel Systems
Analysis Activity
ATTN: AMXSY-MP (H. Cohen)
APG, MD 21005-5071

Commander
U.S. Army Chemical Rsch,
Dev & Engr Center
ATTN: SMCCR-OPA (Ronald Pennsyle)
APG, MD 21010-5423

Commander
U.S. Army Chemical Rsch,
Dev & Engr Center
ATTN: SMCCR-RS (Mr. Joseph Vervier)
APG, MD 21010-5423

Commander
U.S. Army Chemical Rsch,
Dev & Engr Center
ATTN: SMCCR-MUC (Mr. A. Van De Wal)
APG, MD 21010-5423

Director
U.S. Army Materiel Systems
Analysis Activity
ATTN: AMXSY-AT (Mr. Fred Campbell)
APG, MD 21005-5071

Director
U.S. Army Materiel Systems
Analysis Activity
ATTN: AMXSY-CR (Robert N. Marchetti)
APG, MD 21005-5071

Director
U.S. Army Materiel Systems
Analysis Activity
ATTN: AMXSY-CS (Mr. Brad W. Bradley)
APG, MD 21005-5071

Director
U.S. Army Research Laboratory
ATTN: AMSRL-D
2800 Powder Mill Road
Adelphi, MD 20783

Director
U.S. Army Research Laboratory
ATTN: AMSRL-OP-CI-A
(Technical Publishing)
2800 Powder Mill Road
Adelphi, MD 20783

Director
U.S. Army Research Laboratory
ATTN: AMSRL-OP-CI-AD, Record Copy
2800 Powder Mill Road
Adelphi, MD 20783

Director
U.S. Army Research Laboratory
ATTN: AMSRL-SS-SH
Dr. Z.G. Sztankay
2800 Powder Mill Road
Adelphi, MD 20783

National Security Agency
ATTN: W21 (Dr. Longbothum)
9800 Savage Road
Ft George G. Meade, MD 20755-6000

U. S. Army Space Technology
and Research Office
ATTN: Brenda Brathwaite
5321 Riggs Road
Gaithersburg, MD 20882

OIC-NAVSWC
Technical Library (Code E-232)
Silver Springs, MD 20903-5000

The Environmental Research
Institute of Michigan
ATTN: IRIA Library
P.O. Box 134001
Ann Arbor, MI 48113-4001

Commander
U.S. Army Research Office
ATTN: DRXRO-GS (Dr. W.A. Flood)
P.O. Box 12211
Research Triangle Park, NC 27709

Dr. Jerry Davis
North Carolina State University
Department of Marine, Earth, &
Atmospheric Sciences
P.O. Box 8208
Raleigh, NC 27650-8208

Commander
U. S. Army CECRL
ATTN: CECRL-RG (Dr. H. S. Boyne)
Hanover, NH 03755-1290

Commanding Officer
U.S. Army ARDEC
ATTN: SMCAR-IMI-I, Bldg 59
Dover, NJ 07806-5000

U.S. Army Communications-Electronics
Command EW/RSTA Directorate
ATTN: AMSEL-RD-EW-OP
Fort Monmouth, NJ 07703-5206

Commander
U.S. Army Satellite Comm Agency
ATTN: DRCPM-SC-3
Fort Monmouth, NJ 07703-5303

6585th TG (AFSC)
ATTN: RX (CPT Stein)
Holloman AFB, NM 88330

Department of the Air Force
OL/A 2nd Weather Squadron (MAC)
Holloman AFB, NM 88330-5000

PL/WE
Kirtland AFB, NM 87118-6008

Director
U.S. Army TRADOC Analysis Command
ATTN: ATRC-WSS-R
White Sands Missile Range, NM 88002

USAF Rome Laboratory Technical
Library, FL2810 Corridor W, Site 262,
RL//SUL (DOCUMENTS LIBRARY)
26 Electronics Parkway, Bldg 106
Griffiss AFB, NY 13441-4514

AFMC/DOW
Wright-Patterson AFB, OH 0334-5000

Commandant
U.S. Army Field Artillery School
ATTN: ATSF-TSM-TA
Mr. Charles Taylor
Fort Sill, OK 73503-5600

Commander
Naval Air Development Center
ATTN: Al Salik (Code 5012)
Warminister, PA 18974

Commander
U.S. Army Dugway Proving Ground
ATTN: STEDP-MT-DA-M
Mr. Paul Carlson
Dugway, UT 84022

Commander
U.S. Army Dugway Proving Ground
ATTN: STEDP-MT-DA-L
Dugway, UT 84022

Commander
U.S. Army Dugway Proving Ground
ATTN: STEDP-MT-M (Mr. Bowers)
Dugway, UT 84022-5000

Defense Technical Information Center
ATTN: DTIC-FDAC (2)
Cameron Station
Alexandria, VA 22314

Commanding Officer
U.S. Army Foreign Science &
Technology Center
ATTN: CM
220 7th Street, NE
Charlottesville, VA 22901-5396

Naval Surface Weapons Center
Code G63
Dahlgren, VA 22448-5000

Commander
U.S. Army OEC
ATTN: CSTE-EFS
Park Center IV
4501 Ford Ave
Alexandria, VA 22302-1458

Commander and Director
U.S. Army Corps of Engineers
Engineer Topographics Laboratory
ATTN: ETL-GS-LB
Fort Belvoir, VA 22060

TAC/DOWP
Langley AFB, VA 23665-5524

U.S. Army Topo Engineering Center
ATTN: CETEC-ZC
Fort Belvoir, VA 22060-5546

Commander
Logistics Center
ATTN: ATCL-CE
Fort Lee, VA 23801-6000

Commander
USATRADOC
ATTN: ATCD-FA
Fort Monroe, VA 23651-5170

Science and Technology
101 Research Drive
Hampton, VA 23666-1340

Commander
U.S. Army Nuclear & Cml Agency
ATTN: MONA-ZB Bldg 2073
Springfield, VA 22150-3198